FEBS Letters 585 (2011) 511–516

FEBS Letters
journal homepage: www.FEBSLetters.org

Structural characterization of intracellular C-terminal domains of group III metabotropic glutamate receptors

Angela Seebahn [a], Holger Dinkel [a], Jeannine Mohrlüder [b], Rudolf Hartmann [b], Nico Vogel [a], Cord-Michael Becker [a], Heinrich Sticht [a], Ralf Enz [a,*]

[a] Institut für Biochemie (Emil-Fischer-Zentrum), Friedrich-Alexander-Universität Erlangen-Nürnberg, 91045 Erlangen, Germany
[b] Institut für Strukturbiologie und Biophysik 3 (Strukturbiochemie), Forschungszentrum Jülich, 52425 Jülich, Germany

ARTICLE INFO

Article history:
Received 5 November 2010
Revised 27 December 2010
Accepted 28 December 2010
Available online 8 January 2011

Edited by Christian Griesinger

Keywords:
G-protein coupled receptor
Metabotropic glutamate receptor
Neurotransmitter receptor
Short linear motif

ABSTRACT

Metabotropic glutamate receptors (mGluRs) are regulated by interacting proteins that mostly bind to their intracellular C-termini. Here, we investigated if mGluR6, mGluR7a and mGluR8a C-termini form predefined binding surfaces or if they were rather unstructured. Limited tryptic digest of purified peptides argued against the formation of stable globular folds. Circular dichroism, ^{1}H NMR and $^{1}H^{15}N$ HSQC spectra indicated the absence of rigid secondary structure elements. Furthermore, we localized short linear binding motifs in the unstructured receptor domains. Our data provide evidence that protein interactions of the analyzed mGluR C-termini are mediated rather by short linear motifs than by preformed folds.

1. Introduction

Glutamate is the major excitatory neurotransmitter in the central nervous system, acting on ionotropic (ion channel-associated) and metabotropic (G-protein-coupled) glutamate receptors. Metabotropic glutamate receptors (mGluRs) are subdivided into three groups and regulate intracellular signal cascades that modulate neuronal excitability, synaptic plasticity, memory function and neurodegeneration [1]. Group III receptors (mGluR4, mGluR6-8) are negatively coupled to adenylyl cyclase and, with the exception of mGluR6, are suggested to function as presynaptic auto-receptors and low-pass filters [1,2].

Neurotransmission requires a tightly controlled interplay between synaptic proteins, both in space and time. This is accomplished by the formation of synaptic signal complexes that integrate functionally related proteins such as neurotransmitter receptors, enzymes and scaffold proteins. The highest variability between mGluR types is present within their intracellular C-terminal domains and indeed, most described mGluR binding proteins interact with these C-termini (CT) [3]. Importantly, mutations in mGluR binding proteins can lead to neuropsychiatric disorders including addiction, depression, epilepsy and schizophrenia [4].

While the three-dimensional structure of several mGluR binding partners is known, the conformation of the mGluR-CT themselves is poorly characterized. Thus, it is not clear if mGluR-CT contain predefined binding surfaces for interacting proteins, or if these domains are rather unstructured. Therefore, in this study we analyzed the structure of these domains combining biochemical, biophysical and bioinformatic methods.

2. Materials and methods

2.1. Peptide preparation

C-termini of mGluR6, mGluR7a and mGluR8a from rat (Fig. 1) were tagged with glutathione-S-transferase by cloning in pET-41a, expressed in *Escherichia coli* and immobilized on glutathione-Sepharose under native conditions, as described [5]. Peptides were released into the supernatant with Enterokinase (8 U; Novagen, Darmstadt, Germany) for 18 h at 21 °C and analyzed by SERVA-Blue stained Tricine-SDS gels. Because of major side products, the mGluR7a-CT was chemically synthesized with its N-terminus acetylated (AG Henklein, Charité Berlin, Germany).

Abbreviations: CD, circular dichroism; CT, C-terminus; DPC, dodecylphosphocholine; FHA, forkhead associated; HSQC, heteronuclear single quantum coherence; ITSM, immunoreceptor tyrosine-based switch motif; MALDI-TOF, matrix-assisted laser desorption/ionization time-of-flight; mGluR, metabotropic glutamate receptor; NMR, nuclear magnetic resonance; PAH, paired amphiphatic helix; PP1, protein phosphatase 1; SH2/3, Src-homology 2/3; SLiM, short linear motif

* Corresponding author. Fax: +49 9131/852 2485.
E-mail address: ralf.enz@biochem.uni-erlangen.de (R. Enz).

0014-5793/$36.00
doi:10.1016/j.febslet.2010.12.042

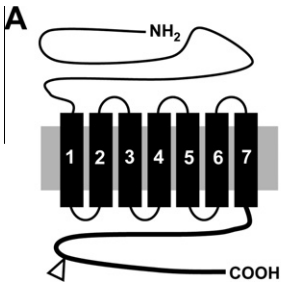

B

Receptor	Source	Weight	Sequence
mGluR6 - CT	E. coli	3.72 kDa	**S**HPEQNVQKRKRSLKKTSTMAAPPQNENAEDAK
mGluR7a-CT	chemical synthesis	7.25 kDa	HPELNVQKRKRSFKAVVTAATMSSRLSHKPSDRPNGEAKTELCENVDP NSPAAKKKYVSYNNLVI
mGluR8a-CT	E. coli	7.39 kDa	**S**HPEQNVQKRKRSFKAVVTAATMQSKLIQKGNDRPNGEVKSELCESLE TNTSSTKTTYISYSNHSI

Fig. 1. Amino acid sequences of mGluR C-termini used in this study. (A) Membrane topology of mGluRs. A grey box represents the membrane, transmembrane regions 1–7 are indicated by black rectangles. The intracellular C-terminus (bold) is alternatively spliced (triangle). (B) Sequences of mGluR-CT generated for this study. Serine residues encoded by the polylinker sequence of the expression vector that remain after Enterokinase cleavage are highlighted in bold. Except for underlined amino acids in mGluR7a, all sequences were predicted to be disordered.

For further purification of mGluR6-CT and mGluR8a-CT, the flow-through from centrifugal filter devices (Millipore, Billerica, MA) with molecular weight cut-offs of 30 kDa (mGluR6) and 50 kDa (mGluR8a) was dialyzed against 20 mM sodium phosphate buffer (pH 7.4) which yielded 500 µl of 80 µM mGluR6-CT and 40 µM mGluR8a-CT. To obtain ^{15}N isotopically labeled mGluR8a-CT, M9 minimal medium with $^{15}NH_4Cl$ (Euriso-top, Saint-Aubin Cedex, France) as sole nitrogen source was used.

2.2. Mass spectrometry

Purified mGluR-CT were prepared for matrix-assisted laser desorption/ionization time-of-flight (MALDI-TOF) mass spectrometry performed on an Autoflex (Bruker Daltonics, Bremen, Germany) in the positive-ion mode as described previously [6]. A peptide standard mix (Bruker Daltonics) served as external calibrant. Fifty individual spectra were averaged and analyzed using the FlexAnalysis software (Bruker Daltonics).

2.3. Limited proteolysis

Hen egg-white lysozyme (0.5 µg/ml in 25 mM NH_4HCO_3; Carl Roth, Karlsruhe, Germany) or mGluR-CT were incubated at 37 °C with trypsin (Promega, München, Germany) at an enzyme to substrate ratio of 1:250. After 10 min, 4 h and 18 h the reaction was quenched with 0.1% trifluoroacetic acid, heated for 5 min at 80 °C, vacuum dried and subjected to MALDI-TOF mass spectrometry. Peak masses were identified by comparing with theoretical masses generated from Protein-Prospector MS Digest (http://prospector.ucsf.edu).

2.4. Circular dichroism (CD) and nuclear magnetic resonance (NMR) techniques

CD spectra of mGluR6-CT (80 µM), mGluR7a-CT (30 µM) and mGluR8a-CT (40 µM) were recorded between 260 nm and 190 nm at 25 °C employing a 0.5 mm cuvette in a Jasco J-810 CD spectrophotometer (Jasco, Groß-Umstadt, Germany). Calculated molar ellipticities were utilized to predict secondary structure elements with CONTINLL and CDSSTR [7]. ^1H NMR spectra of mGluR6-CT (80 µM), mGluR7a-CT (200 µM) and mGluR8a-CT (40 µM) were recorded in the presence of 5% (v/v) D_2O with 256 scans and a recycling time of 3 s at 25 °C using 600 MHz or 800 MHz Unity INOVA spectrometers, equipped with HCN-coldprobes (Varian, Palo Alto, CA), multiplied with a Lorentzian–Gauss window function and Fourier-transformed. $^1H^{15}N$ HSQC spectra were recorded with 8 scans and 128 increments in F1 with or without 50 mM dodecylphosphocholine at 15 °C or 25 °C using the 600 MHz spectrometer, multiplied with a cosine window function in both dimensions and Fourier-transformed.

2.5. Bioinformatic methods

Short linear motifs (SLiMs) were detected by pattern searches [8] using the pattern curated in MiniMotif Miner and the Eukaryotic Linear Motif resource. To estimate the functional relevance of identified motifs, we defined an *E*-value that represents the probability of each motif-associated consensus pattern to be present by chance within any given protein, being low for strictly and high for fuzzy annotated patterns.

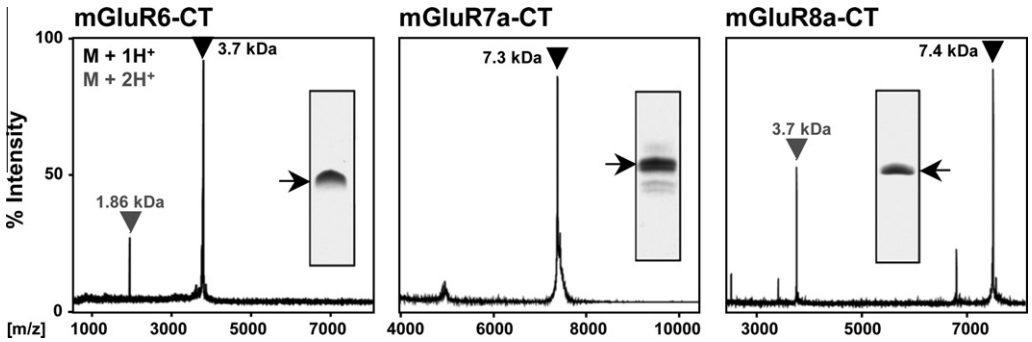

Fig. 2. Characterization of generated mGluR C-termini. MALDI-TOF mass spectra and protein gels (insets) show identity and purity of generated mGluR-CT. Average-isotopic peaks are labeled with observed peptide masses in Dalton. Mass peaks corresponding to mono- or di-protonated masses are marked as $M+1H^+$ (black arrowheads) or $M+2H^+$ (grey arrowheads).

$$E = S * \prod_{i=1}^{m} A_i$$

E depends on the length of the pattern (m) and the fuzziness of its annotation (A). A is the summed frequency of all amino acids allowed at the respective pattern position. S is defined as $S = p - (m + 1)$ using a reference sequence length (p) of 360 amino acids calculated according to the NCBI non-redundant database. S was set to 1 for patterns which occur at N- or C-termini only. To avoid inclusion of non-functional motifs, patterns resulting in E-values of >3 were excluded.

3. Results

3.1. C-termini of mGluR6, mGluR7a and mGluR8a do not form stable globular folds

Computer programs designed to detect natively disordered protein regions [9] predicted the C-terminal domains of mGluR6, mGluR7a and mGluR8a to be mostly unstructured (Fig. 1). However, supporting experimental data is lacking. To test these predictions experimentally, the respective domains were purified under native conditions (mGluR6, mGluR8a) or chemically synthesized (mGluR7a). Size and purity of obtained peptides were analyzed on protein gels and by MALDI-TOF mass spectrometry (Fig. 2). Detected masses were in agreement with calculated molecular weights shown in Fig. 1B, ensuring the identity of generated peptides.

Protease susceptibility can indicate unstructured protein sequences, because globular proteins are usually better protected from proteolytic degradation. Thus, we compared limited proteolysis patterns between the mGluR7a-CT and lysozyme, a protein of comparable size and known globular structure. All trypsin cleavage sites predicted in the mGluR7a-CT were used within 10 min, as evident from resulting cleavage products (mass peaks labeled with asterisks in Fig. 3). Complete digestion was observed after 4 h, while lysozyme was nearly resistant to trypsin digest up to 4 h and only partially degraded after 18 h (Fig. 3). Similar results were obtained for mGluR6-CT and mGluR8a-CT (not shown), indicating that the analyzed mGluR-CT do not form stable globular structures.

3.2. C-termini of mGluR6, mGluR7a and mGluR8a exist in a random coiled conformation

Next, we analyzed the content of secondary structure elements within the mGluR6-CT, mGluR7a-CT and mGluR8a-CT by CD. Molar ellipticities of all CD spectra reached a minimum between 195 nm and 200 nm, indicative of a high degree of random coiled regions (Fig. 4A, dashed lines). In addition, negative ellipticities between 215 nm and 220 nm suggested some amount of extended β-sheet conformations. Superimposure of back calculated curves indicate that the minima were fitted with high quality (Fig. 4A, dotted lines), while some deviations are visible above 210 nm, most evident for mGluR6. Consequently, we refrained from a quantitative analysis of secondary structure elements and conclude that the analyzed mGluR-CT contain a large amount of random coil.

The interpretation of the CD spectra was supported by ^{1}H NMR analysis (Fig. 4B). Specific features suggesting a mainly random coiled structure are (i) the low dispersion of peaks derived from amide protons of the peptide backbone between the region around 8 ppm towards 10 ppm and (ii) the absence of discrete chemical shifts derived from methyl group protons towards 0 ppm. For heteronuclear NMR experiments we generated ^{15}N labeled

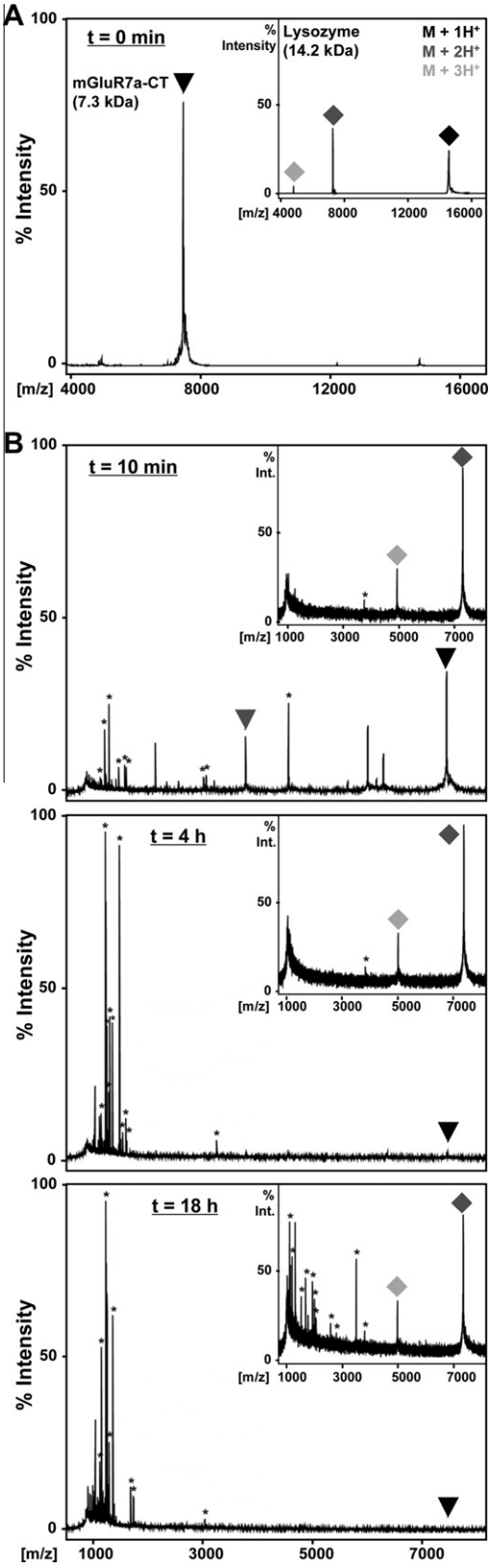

Fig. 3. Limited proteolysis of the mGluR7a C-terminus. MALDI-TOF mass spectra of the undigested mGluR7a-CT (A) and after trypsin digest for the times indicated (B). Lysozyme served as globular control protein (insets). Mono-, di- and tri-protonated masses are distinguished by black, grey and light grey colored arrowheads (mGluR7a-CT) or squares (lysozyme). To reliably separate masses of trypsin-cleaved peptides (asterisks), the x-axis in (B) is shifted towards smaller masses in respect to (A).

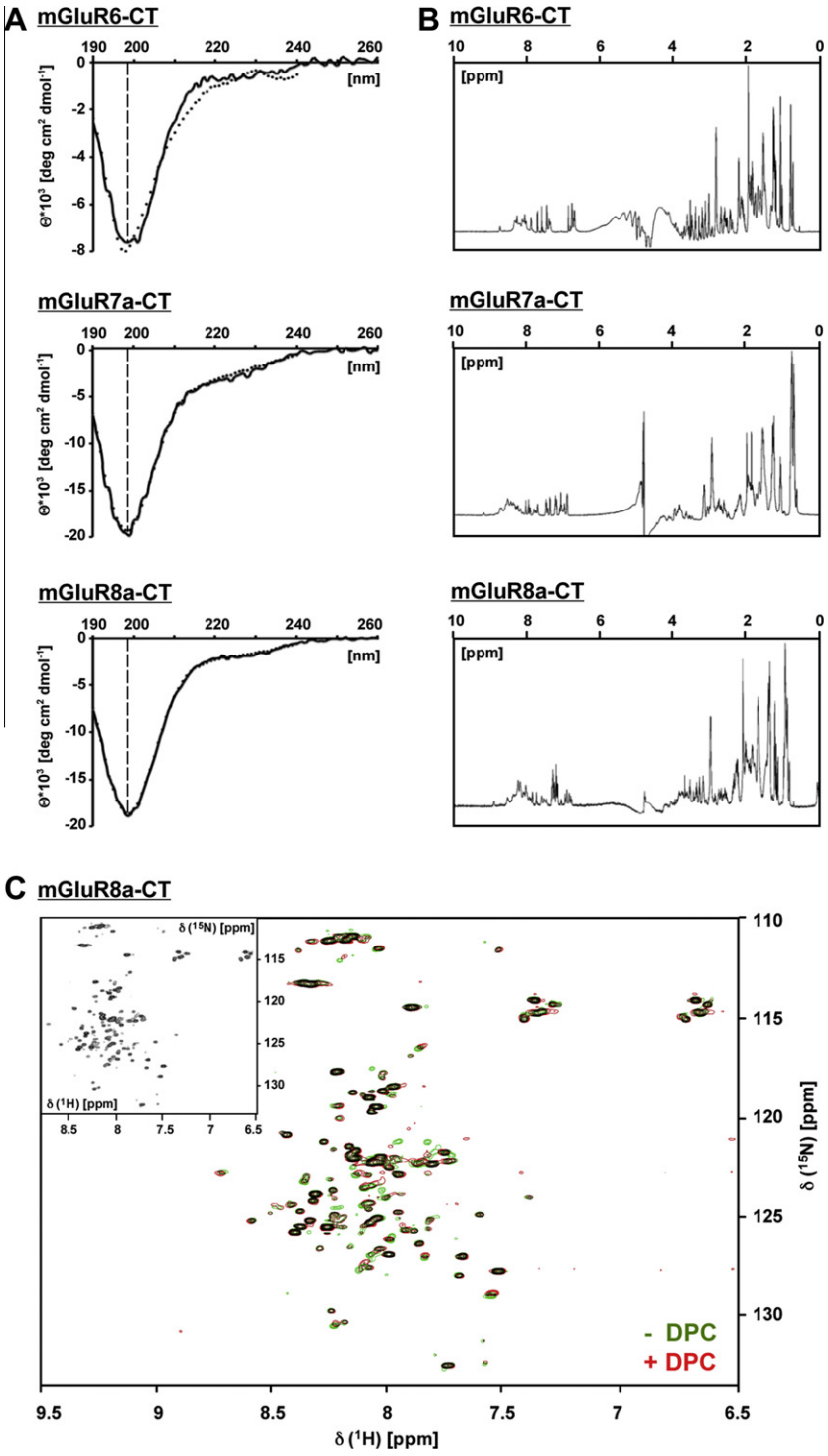

Fig. 4. CD and ^{1}H NMR spectra of mGluR C-termini. (A) Molar ellipticities (Θ) were recorded between 190 nm and 260 nm. Dashed lines indicate a minimum around 198 nm. Back calculated curves are overlaid as dotted lines. (B) ^{1}H NMR spectra reveal a low dispersion of chemical shifts towards 0 or 10 ppm. (C) $^{1}H^{15}N$ HSQC spectra of the mGluR8a-CT recorded at 15 °C (inset) and as overlay with a spectra recorded in the presence of dodecylphosphocholine (DPC; large panel) indicate conformational heterogeneity that is not significantly changed in the presence of lipids. Similar spectra were obtained at 25 °C (not shown).

peptides, however only the mGluR8a-CT was obtained in sufficient amount and purity from minimal medium. Recorded $^{1}H^{15}N$ HSQC spectra revealed more resonances than expected for a peptide containing 65 amino acids (Fig. 4C, inset), indicating that the mGluR8a-CT adopts different spatial structures leading to conformational heterogeneity. MGluR-CT are located close to the membrane and it is possible that they have an affinity for the juxtaposed membrane surface that might induce secondary structures (see Section 4). However, comparison of spectra recorded in the absence or presence of dodecylphosphocholine to mimic possible effects of the lipid bilayer on the mGluR8a-CT structure did not show significant differences (Fig. 4C). These data suggest that the analyzed mGluR-CT do not adopt defined structures that remain stable over time.

A

Domain	Motif Pattern
14-3-3	[RHK][STALV]x [ST]x[PESRDIF]
BRCT	xSxxF
Cyclin A	RxL
FHA	TxxI
ITSM	[VI]xYxx[LV]
PAH2 *	[FA]x[LA][LV][LVI] xx[AM]
PDZ *	[VILMFWYAPHRK] x[VILMFWYAP]$
PP1 *	xx[RK]x(0,1)[VI]{P} [FW]
SH2	YxNx
SH2'	YxxP
SH3	PxxP
Sumo *	[VILMAFP]KxE
WD40	SxxxS
WW	xxx[ST]Px

B

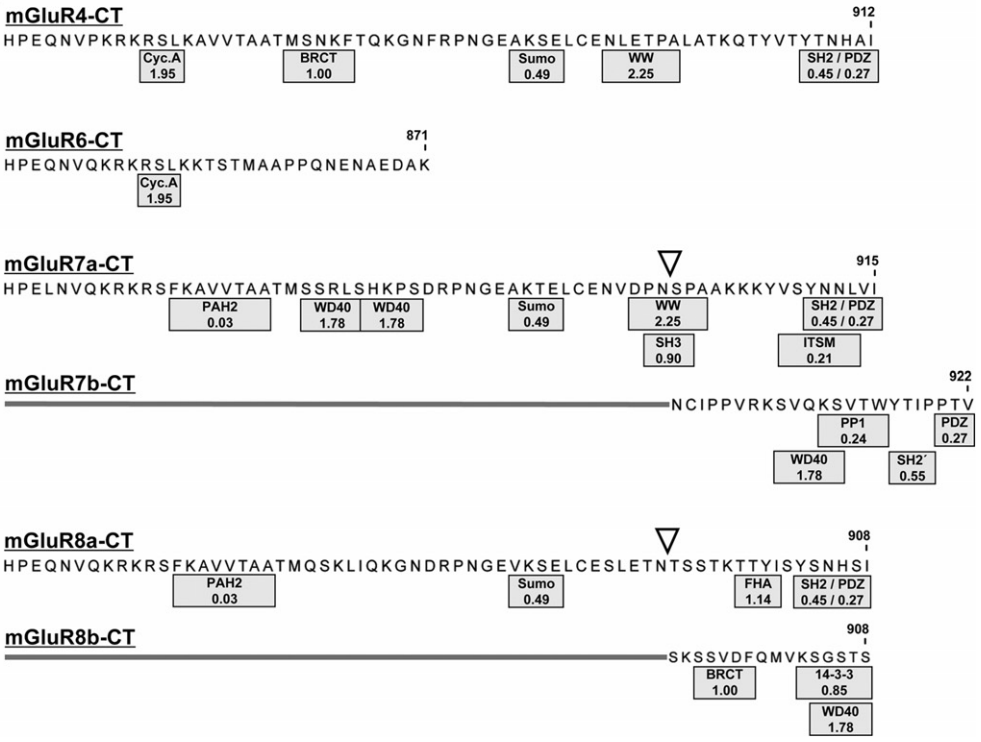

Fig. 5. Prediction of short linear motifs within group III mGluR C-termini. (A) Motif patterns of identified SLiMs within group III mGluR-CT and corresponding interacting domains (or proteins). Asterisks mark interactions which were shown experimentally to be functional. (B) The localization of SLiMs is indicated by grey boxes including calculated *E*-values that estimate their functional relevance (see methods for details). For clarity, motifs for posttranslational modifications, protein trafficking and protease cleavage sites are not shown. Alternative splicing in mGluR-CT is indicated by triangles.

3.3. Identification of short linear motifs within group III mGluR C-termini

Protein–protein interaction may not only occur between globular domains; alternatively a globular domain in one protein may also recognize short stretches of approximately three to ten residues in the binding partner. These regions often show a particular sequence pattern, or short linear motif (SLiM), which contains the key residues involved in function or binding. Binding via SLiMs is estimated to account for 15–40% of the interactions in the human proteome and occur more often in disordered rather than ordered protein regions [10].

Indeed, pattern search algorithms predicted several SLiMs in group III mGluR-CT (Fig. 5). Calculated *E*-values estimate the functional relevance of identified motifs (Fig. 5B; see methods for details). Except for one threonine to alanine exchange in the mGluR4 WW domain, the shown SLiMs are evolutionary conserved between rat, mouse and human, underscoring the validity of our predictions. In conclusion, the presence of several linear interaction motifs in group III mGluR-CT supports our experimental observations that these domains are largely disordered.

4. Discussion

In addition to the well-established concept that structure determines function, evidence for the biological importance of intrinsically disordered protein regions is increasing (e.g. reviewed in [9]). It was estimated that about 70% of signaling proteins contain unstructured regions, enabling them to form overlapping binding motifs that contact multiple interactors. The physiological significance of disordered regions is underlined by their association with human diseases, including Alzheimer's and Parkinson's disease and thus, they represent interesting drug targets [9].

Here, we characterized C-termini of mGluR6, mGluR7a and mGluR8a to be largely disordered. Other than the globular control protein lysozyme, the mGluR-CT were completely digested by trypsin after 4 h. The number of trypsin cleavage sites per amino acid in lysozyme and the receptor peptides are comparable (0.13–0.15), indicating that the accessibility for trypsin is low in lysozyme and high in mGluR-CT, pointing towards an unorganized structure of these domains. This is consistent with our CD and NMR measurements that show mainly random coiled conformations. However, based on our experiments we cannot completely rule out the existence of short regions of regular secondary structure, especially if these elements form for short time periods.

The disordered nature of analyzed mGluR-CT suggested the presence of short linear motifs for protein–protein interactions and indeed, we localized several SLiMs in these domains. For several motifs, interacting proteins have already been identified from experiment, ensuring the reliability of the algorithms. Consistent with our predictions, the PDZ domain of PICK1 and the Sumo E3-ligase Pias1 interacted with several mGluR-CT, while protein phosphatase 1 (PP1) bound to mGluR7b [3]. The most probable SLiM detected is the binding motif for PAH2 domains with an *E*-value of 0.03. Indeed, an amphipathic α-helix is induced by Calmodulin upon interacting with this region in the mGluR7a-CT [11]. Because domains binding to other identified SLiMs are present in several proteins (e.g. SH3 domains are present in over 700 human proteins), the experimental identification of physiological interactors for these motifs is outside the scope of this manuscript.

Unstructured mGluR-CT might contain the intrinsic capability to adopt defined secondary structures upon binding interacting

proteins. This hypothesis is supported by experimental data: The mGluR7a-CT forms an amphipathic α-helix in contact with Calmodulin, while 5 amino acids of the mGluR7b-CT adopt an extended β-sheet conformation in complex with PP1 [5,11]. Alternatively, regions of ordered structure within mGluR-CT might be induced by close proximity to the lipid bilayer. Indeed, a lipid-induced α-helix was proposed e.g. in the cannabinoid receptor 1 C-terminus and crystal structures of β-adrenergic receptors show a C-terminal α-helix orientated parallel to the lipid bilayer [12,13]. In contrast, we did not observe significant changes in the mGluR8a-CT after addition of dodecylphosphocholine in heteronuclear NMR experiments, arguing against a lipid-induced helix. Although different expression levels of mGluR-CT in minimal medium allowed to record $^{1}H^{15}N$ HSQC spectra from the mGluR8a-CT only, the qualitatively highly similar CD and ^{1}H NMR spectra presented for the mGluR6-CT, mGluR7a-CT and mGluR8a-CT suggest similar structural properties of these peptides, indicating that all three mGluR-CT analyzed remain disordered in the presence of lipids.

Regions of ordered structure within mGluR-CT might also be favored by the vicinity of other receptor domains. However, studies describing crystal structures of G-protein coupled receptors for glutamate, adrenaline or adenosine excluded intracellular domains [14,15], suggesting a high flexibility of these regions, being consistent with our data. The observed absence of detectable structure in the analyzed mGluR-CT are also in agreement with folding characteristics of ionotropic receptors for glutamate or acetylcholine [16,17], pointing towards a general feature of intracellular domains of neurotransmitter receptors.

Acknowledgments

We thank Wei Xiang for help with mass spectrometry and Dieter Willbold for helpful discussions. This work was supported by the Deutsche Forschungsgemeinschaft [EN349/5-2, EU-HEALTH-F4-2008-202088, SFB539, SFB796].

References

[1] Ferraguti, F. and Shigemoto, R. (2006) Metabotropic glutamate receptors. Cell Tissue Res. 326, 483–504.
[2] Schoepp, D.D. (2001) Unveiling the functions of presynaptic metabotropic glutamate receptors in the central nervous system. J. Pharmacol. Exp. Ther. 299, 12–20.
[3] Enz, R. (2007) The trick of the tail: protein–protein interactions of metabotropic glutamate receptors. Bioassays 29, 60–73.
[4] Szumlinski, K.K., Kalivas, P.W. and Worley, P.F. (2006) Homer proteins: implications for neuropsychiatric disorders. Curr. Opin. Neurobiol. 16, 251–257.
[5] Croci, C., Sticht, H., Brandstätter, J.H. and Enz, R. (2003) Group I metabotropic glutamate receptors bind to protein phosphatase 1C. Mapping and modeling of interacting sequences. J. Biol. Chem. 278, 50682–50690.
[6] Ulrich, M., Seeber, S., Becker, C.M. and Enz, R. (2007) Tax1-binding protein 1 is expressed in the retina and interacts with the GABA(C) receptor rho1 subunit. Biochem. J. 401, 429–436.
[7] Whitmore, L. and Wallace, B.A. (2004) DICHROWEB, an online server for protein secondary structure analyses from circular dichroism spectroscopic data. Nucleic Acids Res. 32, W668–W673.
[8] Dinkel, H. and Sticht, H. (2007) A computational strategy for the prediction of functional linear peptide motifs in proteins. Bioinformatics 23, 3297–3303.
[9] Uversky, V.N. and Dunker, A.K. (2010) Understanding protein non-folding. Biochim. Biophys. Acta 1804, 1231–1264.
[10] Ren, S., Uversky, V.N., Chen, Z., Dunker, A.K. and Obradovic, Z. (2008) Short Linear Motifs recognized by SH2, SH3 and Ser/Thr kinase domains are conserved in disordered protein regions. BMC Genomics 9 (Suppl. 2), S26.
[11] Scheschonka, A. et al. (2008) Structural determinants of calmodulin binding to the intracellular C-terminal domain of the metabotropic glutamate receptor 7 Å. J. Biol. Chem. 283, 5577–5588.
[12] Ahn, K.H., Pellegrini, M., Tsomaia, N., Yatawara, A.K., Kendall, D.A. and Mierke, D.F. (2009) Structural analysis of the human cannabinoid receptor one carboxyl-terminus identifies two amphipathic helices. Biopolymers 91, 565–573.
[13] Rasmussen, S.G. et al. (2007) Crystal structure of the human beta2 adrenergic G-protein-coupled receptor. Nature 450, 383–387.
[14] Muto, T., Tsuchiya, D., Morikawa, K. and Jingami, H. (2007) Structures of the extracellular regions of the group II/III metabotropic glutamate receptors. Proc. Natl. Acad. Sci. USA 104, 3759–3764.
[15] Rosenbaum, D.M., Rasmussen, S.G. and Kobilka, B.K. (2009) The structure and function of G-protein-coupled receptors. Nature 459, 356–363.
[16] Kukhtina, V., Kottwitz, D., Strauss, H., Heise, B., Chebotareva, N., Tsetlin, V. and Hucho, F. (2006) Intracellular domain of nicotinic acetylcholine receptor: the importance of being unfolded. J. Neurochem. 97 (Suppl. 1), 63–67.
[17] Sobolevsky, A.I., Rosconi, M.P. and Gouaux, E. (2009) X-ray structure, symmetry and mechanism of an AMPA-subtype glutamate receptor. Nature 462, 745–756.